European Journal of Medicinal Chemistry 183 (2019) 111671

Contents lists available at ScienceDirect

European Journal of Medicinal Chemistry

journal homepage: http://www.elsevier.com/locate/ejmech

Research paper

Antimicrobial activity of amphipathic α,α-disubstituted β-amino amide derivatives against ESBL − CARBA producing multi-resistant bacteria; effect of halogenation, lipophilicity and cationic character

Marianne H. Paulsen [a], Dominik Ausbacher [a, f], Annette Bayer [b, **], Magnus Engqvist [b], Terkel Hansen [a], Tor Haug [c], Trude Anderssen [a], Jeanette H. Andersen [d], Johanna U. Ericson Sollid [e], Morten B. Strøm [a, *]

[a] Department of Pharmacy, Faculty of Health Sciences, UiT − The Arctic University of Norway, NO-9037, Tromsø, Norway
[b] Department of Chemistry, Faculty of Science and Technology, UiT − The Arctic University of Norway, NO-9037, Tromsø, Norway
[c] The Norwegian College of Fishery Science, Faculty of Biosciences, Fisheries and Economics, UiT − The Arctic University of Norway, NO-9037, Tromsø, Norway
[d] Marbio, Faculty of Biosciences, Fisheries and Economics, UiT − The Arctic University of Norway, NO-9037, Tromsø, Norway
[e] Department of Medical Biology, Faculty of Health Sciences, UiT − The Arctic University of Norway, NO-9037, Tromsø, Norway
[f] Hospital Pharmacy of North Norway Trust, NO-9038, Tromsø, Norway

ARTICLE INFO

Article history:
Received 27 June 2019
Received in revised form
27 August 2019
Accepted 30 August 2019
Available online 6 September 2019

Keywords:
Antibacterial
Antimicrobial peptides
Beta-amino acids
ESBL
CARBA
Multi-resistant bacteria
Peptidomimetics
SMAMPs
Synthetic mimics of antimicrobial peptides

ABSTRACT

The rapid emergence and spread of multi-resistant bacteria have created an urgent need for new antimicrobial agents. We report here a series of amphipathic α,α-disubstituted β-amino amide derivatives with activity against 30 multi-resistant clinical isolates of Gram-positive and Gram-negative bacteria, including isolates with extended spectrum β-lactamase − carbapenemase (ESBL-CARBA) production. A variety of halogenated aromatic side-chains were investigated to improve antimicrobial potency and minimize formation of Phase I metabolites. Net positive charge and cationic character of the derivatives had an important effect on toxicity against human cell lines. The most potent and selective derivative was the diguanidine derivative **4e** with 3,5-di-brominated benzylic side-chains. Derivative **4e** displayed minimum inhibitory concentrations (MIC) of 0.25−8 μg/mL against Gram-positive and Gram-negative reference strains, and 2−32 μg/mL against multi-resistant clinical isolates. Derivative **4e** showed also low toxicity against human red blood cells ($EC_{50} > 200$ μg/mL), human hepatocyte carcinoma cells (HepG2: $EC_{50} > 64$ μg/mL), and human lung fibroblast cells (MRC-5: $EC_{50} > 64$ μg/mL). The broad-spectrum antimicrobial activity and low toxicity of diguanylated derivatives such as **4e** make them attractive as lead compounds for development of novel antimicrobial drugs.

1. Introduction

Modern society is facing the reality of a post-antibiotic era due to the rapid emergence and spread of multi-resistant bacteria and the lack of new antibiotics. European health authorities have estimated that more than 33 000 patients die of infections caused by multi-resistant bacteria each year, despite the use of considerable financial resources of more than 1.5 billion Euros annually [1–3]. The European Union started the Innovative Medicine Initiative (IMI) in 2008, the largest public private partnership worldwide in order to facilitate and accelerate the development of better medicines [4]. Other initiatives have also been launched to tackle the scientific, regulatory, and business challenges that hamper the development of new antibiotics [5].

Aware of the increasing need of innovative antibiotics, our group is developing and investigating amphipathic peptidomimetics such as small α,α-disubstituted β-amino amides as potential antimicrobial agents, and for applications against microbial biofilms or cancer [6–11]. The structural design of these compounds is inspired by cationic antimicrobial peptides (AMPs), which are a crucial part of innate immunity in virtually every eukaryotic species [12]. Natural

* Corresponding author.
** Corresponding author.
E-mail addresses: annette.bayer@uit.no (A. Bayer), morten.strom@uit.no (M.B. Strøm).

https://doi.org/10.1016/j.ejmech.2019.111671

AMPs are usually positively charged (+2 to +9), amphipathic, consist of 12–50 amino acid residues, and interact with bacteria first by electrostatic interactions followed by disruption of bacterial membrane structures [13]. The selectivity of cationic AMPs for bacterial membranes is due to their higher content of negatively charged cell wall components like teichoic acids, cardiolipin, and phosphatidylglycerol, whereas mammalian cell membranes consist of neutrally charged phospholipids and are stabilized by cholesterol [12,14,15].

We have previously reported antimicrobial α,α-disubstituted β-amino amides, which were designed based on the pharmacophore model for short cationic AMPs suggesting that amphipathic peptidomimetics should contain two cationic charged groups and two lipophilic bulky groups as important key features [10,16]. Other examples of peptidomimetics or *synthetic mimics of AMPs* (SMAMPs) exploring similar key features are reported by Teng et al. [17], Ghosh et al. [18], Dewangan et al. [19], Murugan et al. [20], and the groups of Svendsen [21,22], Bang [23], Tew [24–26], and DeGrado [27,28]. The previously reported α,α-disubstituted β-amino amides showed highest preference for Gram-positive bacteria, including antibiotic-resistant strains like methicillin resistant *Staphylococcus aureus* (MRSA) and methicillin resistant *Staphylococcus epidermidis* (MRSE), and biofilm producing strains [6,7]. The *mode-of-action* involves membrane disruption and resembles mechanisms reported for much larger AMPs [6,29]. Furthermore, the α,α-disubstituted β-amino amides are stable against degradation by α-chymotrypsin and stable in aqueous solutions at pH 7.4 [8]. However, α,α-disubstituted β-amino amides are susceptible to Phase I oxidations by murine liver microsomes [30]. Especially electron rich aromatic (2-naphthyl)methyl side-chain groups can be extensively oxidised. A strategy to reduce the possibility of Phase I oxidations was therefore important to address in the present design.

We hereby report the antimicrobial activity of a series of halogenated α,α-disubstituted β-amino amides (**2a**–**i**), where the side-chains were deactivated through halogenation to limit possible Phase I metabolites (Fig. 1). We also included the synthetic monoamine nitrile precursors (**1a**–**i**), a non-halogenated derivative **2j**, triamine derivatives (**3d**, **3e**, **3g**, **3i**), and diguanidine derivatives (**4e**, **4g**, **4i**) in the study. Our aim was to optimize antimicrobial potency and reduce human cell toxicity through modifications of overall lipophilicity, side-chain structures, and net positive charge and basicity. The prepared derivatives were screened for antimicrobial activity against Gram-positive and Gram-negative reference strains, and toxicity was evaluated against human red blood cells (RBCs), human hepatocyte carcinoma cells (HepG2), and human lung fibroblast cells (MRC-5). To further demonstrate their potential as antimicrobial lead compounds, the most promising derivatives were tested against a panel of 30 multi-resistant clinical isolates of MRSA, vancomycin resistant *Enterococci* (VRE), and extended spectrum β-lactamase − carbapenemase (ESBL-CARBA) producing Gram-negative isolates of *Escherichia coli, Pseudomonas aeruginosa, Klebsiella pneumoniae,* and *Acinetobacter baumannii*, which are the main causatives of severe nosocomial infections [31]. Three diamine derivatives (**2e**, **2g**, **2i**) with representative halogenated side-chains were also investigated for possible CYP450 Phase 1 metabolism using murine liver microsomes.

2. Results and discussion

2.1. Synthesis

Synthesis of the monoamine derivatives **1a**–**i** and the diamine derivatives **2a**–**j** were carried out according to our optimized reported method (Scheme 1) [32]. In brief, dialkylation of methyl cyanoacetate with the appropriate benzyl or 1-naphthyl bromides in dichloromethane with 1,8-diazabicyclo[5.4.0]undec-7-ene (DBU) as base gave **5a**–**i**, and was followed by aminolysis with ethylenediamine to give the monoamine derivatives **1a**–**i**. Reduction of monoamines **1a**–**i** with either Raney-Nickel or $ZnCl_2/NaBH_4$ gave the diamine derivatives **2a**–**j** and the triamine derivatives **3d**, **3e**, **3g** and **3i**. Whereas reduction with $ZnCl_2/NaBH_4$ for 1.5 h resulted in the diamine derivatives **2d**, **2e**, and **2i**, longer reduction of the amide functionality for 24 h gave the *over-reduced* triamine derivatives **3d**, **3e**, **3g**, and **3i**. The diguanylated derivatives **4e**, **4g** and **4i** were synthesized from the corresponding diamine salts **2** by treatment with K_2CO_3 and *N*,*N*′-Di-Boc-1H-pyrazole-1-carboxamidine in THF. The resulting Boc-protected diguanylated derivatives were then deprotected with TFA in dichloromethane to yield **4e**, **4g** and **4i**.

Based on our previously reported method, reduction of the fluorinated monoamine derivatives was performed with Raney-Nickel providing **2a**–**c**, **2f**–**h**, and **2j**, while the brominated monoamine derivatives had to be reduced with $ZnCl_2/NaBH_4$ to avoid de-bromination [32]. Surprisingly, Raney-Nickel reduction of the 4-fluoronapht-1-yl substituted nitrile **1i** resulted in de-fluorination within 30 min giving **2j** and not the expected diamine derivative **2i**. Fortunately, the de-fluorination was avoided by reducing **1i** to **2i** with $ZnCl_2/NaBH_4$ (1.5 h) similar to the brominated nitriles. In general, the synthesis was scalable and efficient involving only a few chromatographic purification steps.

2.2. Antimicrobial activity against bacterial reference strains and toxicity against human cells

The monoamines **1**, diamines **2**, triamines **3**, and diguanidines **4** (Fig. 1) were first evaluated for antimicrobial activity against Gram-positive and Gram-negative reference strains (Table 1). Toxicity was evaluated against human red blood cells (RBCs), human hepatocyte carcinoma cells (HepG2), and human lung fibroblast cells (MRC-5) (Table 1). The RBC results were also used for calculating a selectivity index (SI) by dividing the RBC EC_{50} value with the minimum inhibitory concentration (MIC) against *S. aureus* or *E. coli*. Derivatives with MIC $\leq$8 μg/mL and SI $\geq$ 10 were considered promising as lead compounds for further investigations. The results revealed MIC values ranging from 0.25 to 4 μg/mL for the most potent monoamine **1**, diamines **2**, triamines **3**, and diguanidines **4** against Gram-positive and Gram-negative bacteria, but considerable variation was observed in haemolytic activity (RBC EC_{50}: 23–>300 μg/mL) and human cell cytotoxicity (HepG2 or MRC-5 EC_{50}: 4–>64 μg/mL), as discussed below. In the following sections abbreviations used for side-chains are included in parentheses to aid the discussion.

2.2.1. Correlation between antimicrobial activity and side-chain size

Screening results for the monoamines **1a-i** (Table 1) revealed a strong correlation between antimicrobial activity and side-chain size showing that the smallest fluorinated derivatives (**1a-c**) were either inactive or much less potent than the larger bromo- and trifluoromethylbenzyl derivatives (**1d**, **1f**–**i**). For the monoamines, **1i** (4-F-1-Nal) displayed highest antimicrobial activity and was potent against all bacterial reference strains tested (MIC: 2–32 μg/mL). The trifluoromethylbenzyl derivatives **1f**–**h** showed comparable antimicrobial activity against the bacterial reference strains (MIC: 8–64 μg/mL) and were more potent than the brominated derivatives **1d**–**e**. Derivative **1d** (2-Br-Ph) displayed antimicrobial activity against the Gram-positive strains and *E. coli* (MIC: 16–32 μg/mL), but was not active against *P. aeruginosa*. A high antimicrobial activity was anticipated for **1e** (3,5-Br-Ph) with larger

Monoamine derivatives – nitrile precursors of the target halogenated α,α-disubstituted β-amino amides ***(1a–i)***

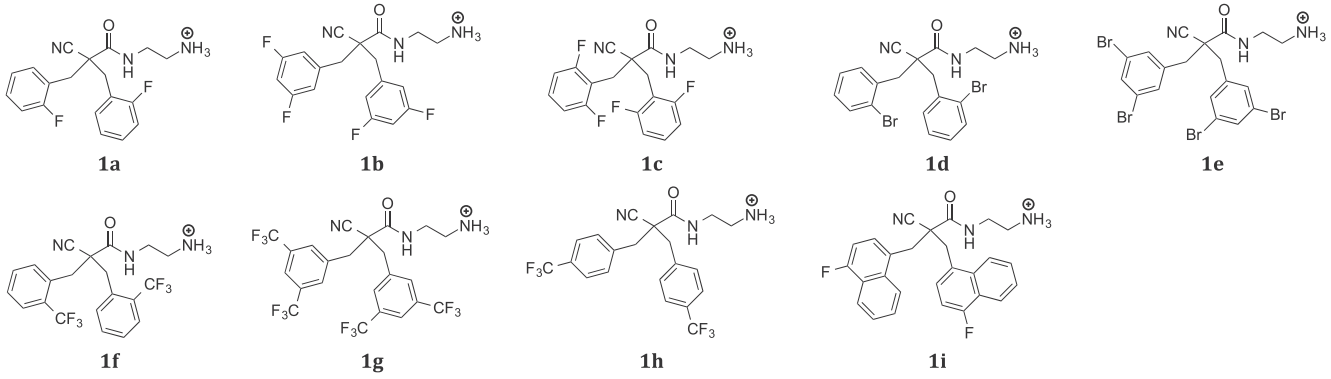

Diamine derivatives – target halogenated α,α-disubstituted β-amino amides ***(2a–j)***

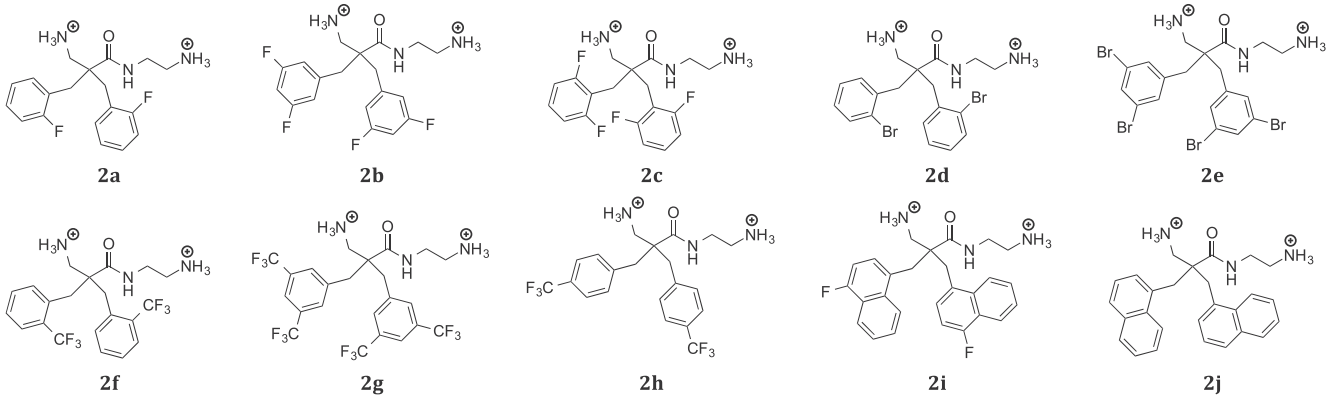

Triamine derivatives – α,α-disubstituted β-amino amines after reduction of the corresponding amino amides ***(3d, 3e, 3g, 3i)***

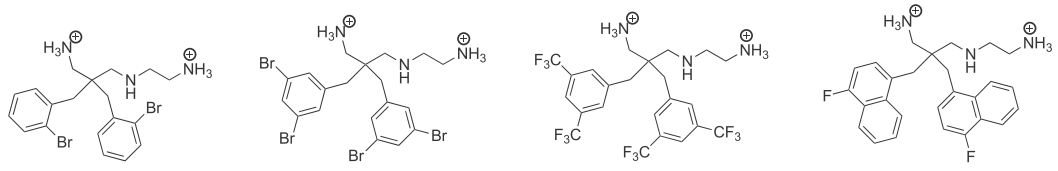

Diguanidine derivatives – optimized diguanylated derivatives of halogenated α,α-disubstituted β-amino amide ***(4e, 4g, 4i)***

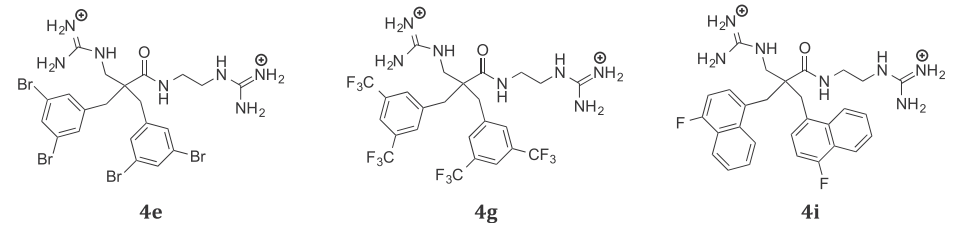

Fig. 1. Structures of the halogenated monoamine nitrile precursors **1a**–**1i**, the target halogenated α,α-disubstituted β-amino amides **2a**–**2i** and the de-fluorinated **2j**, the reduced triamines **3d**, **3e**, **3g** and **3i**, and the optimized diguanidine derivatives (**4e**, **4g**, and **4i**) investigated for antimicrobial activity. Diamine **2j** was a result of de-fluorination during synthesis of **2i**. All derivatives are shown in their expected ionized state at pH 7.4.

side-chains, but **1e** (3,5-Br-Ph) was poorly soluble in aqueous test media, and we were therefore unable to detect any antimicrobial activity (MIC: >64 μg/mL). For the smallest derivatives **1a**–**c** having fluorobenzyl side-chains, **1a** (2-F-Ph) displayed antimicrobial activity against *Corynebacterium glutamicum* and *E. coli*, **1b** (3,5-F-Ph) was only active against *C. glutamicum,* whereas **1c** (2,6-F-Ph) was altogether inactive.

The antimicrobial monoamines **1** showed very low toxicity against RBCs (EC_{50}: ≥178 μg/mL), except for **1f** (2-CF_3-Ph) (EC_{50}: 89 μg/mL) (Table 1). Haemolytic activity for **1i** (4-F-1-Nal) was, however, difficult to determine because of precipitation when PBS was added in the particular RBC assay. The highly potent derivative **1i** (4-F-1-Nal) showed inappropriately high cytotoxicity against HepG2 (EC_{50}: 12 μg/mL) and MRC-5 cells (EC_{50}: 4 μg/mL) and was thereby not sufficiently selective for bacteria compared to human cells to be of interest as a lead compound. The remaining monoamine derivatives were in general less cytotoxic than **1i** (4-F-1-Nal) against HepG2 and MRC-5 cells (EC_{50}: 12–>64 μg/mL). Overall, the combination of low antimicrobial activity, poor selectivity (i.e. low SI except for **1g** (3,5-CF_3-Ph)), and limited aqueous solubility made

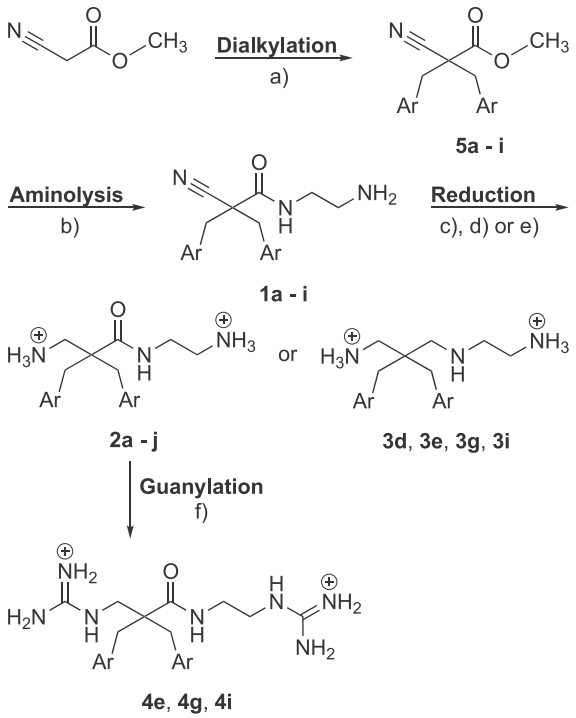

Scheme 1. Synthesis of halogenated monoamine derivatives (**1a**–**i**), α,α-disubstituted β-amino amides (i.e. diamines **2a**–**j**), triamines (**3d**, **3e**, **3g**, **3i**), and diguanidines (**4e**, **4g**, **4i**) investigated for antimicrobial activity. The series included also the de-fluorinated diamine derivative **2j** from the first attempted synthesis of **2i** [32]. Reaction condition: a) Ar–CH_2–Br, DBU, CH_2Cl_2, r.t. b) Ethylenediamine (solvent), r.t., 0.5–24 h. c) For synthesis of **2a**–**c**, **2f**–**h**, and **2j**: 1) Raney-Nickel/H_2(g), Boc_2O, MeOH or EtOAc, 45 °C (18 h), 1 or 8–10 bar, 2) 1.33 M HCl in dioxane, 60 °C (2 h). d) For synthesis of **2d**, **2e**, **2i**: $ZnCl_2$/$NaBH_4$, THF, reflux (1.5 h). e) For synthesis of **3d**, **3e**, **3g**, **3i**: $ZnCl_2$/$NaBH_4$, THF, reflux (24 h). f) K_2CO_3, *N*,*N*′-Di-Boc-1H-pyrazole-1-carboxamidine, THF, r.t. 48–72 h.

the monoamines **1** little attractive as antimicrobial lead compounds. The limited water solubility may be explained by this series having only a single ionisable group to make up for the lipophilic contribution of the side-chains.

2.2.2. Increasing net positive charge and increased antimicrobial potency

Increasing the net positive charge gave a general improvement in antimicrobial activity, as observed for the diamines **2**, and also improved aqueous solubility. The most potent and broad-spectrum derivatives were the bulky side-chain derivatives **2e** (3,5-Br-Ph), **2g** (3,5-CF_3-Ph), and **2i** (4-F-1-Nal) (MIC: 1–8 μg/mL). The effect of side-chain size on antimicrobial activity was thereby further emphasized, as well as the advantage of increasing the net positive charge. The *de-fluorinated* derivative **2j** (1-Nal) displayed similar antimicrobial activity against the Gram-positive strains (MIC: 2–4 μg/mL) as its fluorinated analogue **2i** (4-F-1-Nal), but **2j** (1-Nal) was less potent against the Gram-negative bacteria (MIC: 16 μg/mL).

The previously reported derivative **2h** (4-CF_3-Ph) was in general more potent than the analogous derivative **2f** (2-CF_3-Ph) revealing a positional effect of the CF_3-substituent [6]. As a smaller brominated analogue of **2f** (2-CF_3-Ph), derivative **2d** (2-Br-Ph) was also less potent and showed low antimicrobial activity against all reference strains (MIC: 64 μg/mL) except against *C. glutamicum* (MIC: 8 μg/mL). For the smallest fluorinated derivatives **2a**–**c**, detectable antimicrobial activity was only observed for **2b** (3,5-F-Ph) against *C. glutamicum* (MIC: 64 μg/mL). The results for the diamines **2** demonstrated a favourable antimicrobial effect by increased cationic charge (+2) and bulky steric demanding side-chains, and especially in order to ensure high activity against the Gram-negative bacteria *E. coli* and *P. aeruginosa*.

Toxicity against human RBCs of the most antimicrobial active derivatives **2e** (3,5-Br-Ph), **2g** (3,5-CF_3-Ph) and **2i** (4-F-1-Nal) was higher (EC_{50}: 48–74 μg/mL) than for the other diamines **2** (EC_{50}: 90–312 μg/mL). Derivative **2i** (4-F-1-Nal) was least haemolytic, followed by **2e** (3,5-Br-Ph) and **2g** (3,5-CF_3-Ph), although the differences between these were minimal. The high antimicrobial potencies of **2e**, **2g** and **2i** resulted in SI of 12–29, which was an improvement compared to the antimicrobial monoamines **1** (Table 1). Cytotoxicity of **2e** (3,5-Br-Ph), **2g** (3,5-CF_3-Ph) and **2i** (4-F-1-Nal) against HepG2 (EC_{50}: 11–13 μg/mL) and MRC-5 (EC_{50}: 4–17 μg/mL) cells was, however, unsatisfactory and revealed limited selectivity for bacteria compared to human cells. Derivative **2j** (1-Nal), which was highly potent against the Gram-positive strains, was less toxic against RBCs (EC_{50}: 90 μg/mL) resulted in a SI of 23 with respect to *S. aureus*. Toxicity against MRC-5 cells (EC_{50}: 9 μg/mL) was at the same level as for the most potent diamines and therefore not satisfactory. The previously reported derivative **2h** (4-CF_3-Ph) was practically non-haemolytic (EC_{50}: 289 μg/mL) and resulted in high SI of 18–36. This derivative has not been tested against HepG2, but showed cytotoxicity against MRC-5 cells (EC_{50}: 16 μg/mL). Its CF_3-positional analogue **2f** (2-CF_3-Ph) was less toxic against RBCs (EC_{50}: 312 μg/mL), HepG2 cells (EC_{50}: 45 μg/mL), and MRC-5 cells (EC_{50}: 42 μg/mL) in accordance with having lower antimicrobial activity. The low antimicrobial activity of **2d** (2-Br-Ph) agreed with this derivative being non-haemolytic (EC_{50} 271 μg/mL), and exhibiting low cytotoxicity against HepG2 (EC_{50}: 48 μg/mL) and MRC-5 (EC_{50}: 56 μg/mL) cells. The results thereby demonstrated a structural correlation between antimicrobial activity and toxicity against human cells for the diamines **2**. When evaluating overall broad-spectrum antimicrobial activity and human cell toxicity of the diamines **2**, the three derivatives **2e** (3,5-Br-Ph), **2g** (3,5-CF_3-Ph) and **2i** (4-F-1-Nal) were the most promising candidates from this series, although a higher SI would have been favoured.

2.2.3. Increased haemolytic activity by reduction of the amide group

In an attempt to reduce human cell toxicity, we prepared a small series of triamine derivatives **3d** (2-Br-Ph), **3e** (3,5-Br-Ph), **3g** (3,5-CF_3-Ph), and **3i** (4-F-1-Nal) by *over-reduction* of the corresponding diamine **2** precursors with $ZnCl_2$/$NaBH_4$. This reduction of the amide group allowed us to investigate the influence of an additional amino group, and potentially increased net positive charge, for antimicrobial potency and toxicity (Fig. 1 and Scheme 1). The side-chain motifs were inspired by the most potent diamine derivatives **2e** (3,5-Br-Ph), **2g** (3,5-CF_3-Ph), and **2i** (4-F-1-Nal) and the less potent **2d** (2-Br-Ph). The results showed that **3e** (3,5-Br-Ph), **3g** (3,5-CF_3-Ph), and **3i** (4-F-1-Nal) displayed high and broad-spectrum antimicrobial activity (MIC: 1–4 μg/mL) against all the reference strains. The antimicrobial potencies of these triamine derivatives were thereby in the same range as their diamine counterparts, as observed by pairwise comparing MIC values for **2e**/**3e** (3,5-Br-Ph), **2g**/**3g** (3,5-CF_3-Ph), and **2i**/**3i** (4-F-1-Nal). Derivative **3d** (2-Br-Ph) showed furthermore a fourfold increase in potency against all strains (MIC: 2–16 μg/mL) compared to its diamine counterpart **2d** (2-Br-Ph) (MIC: 8–64 μg/mL). The haemolytic activity was, however, more than 2-fold higher for the triamine derivatives **3e** (3,5-Br-Ph), **3g** (3,5-CF_3-Ph), and **3i** (4-F-1-Nal) compared to the diamine derivatives, whereas cytotoxicity against HepG2 and MRC-5 was less affected. An exception was the triamine derivative **3d** (2-Br-Ph), which showed only a small increase in RBC toxicity (EC_{50}: 209 μg/mL), but a more drastic increase in HepG2

Table 1
Antimicrobial activity (MIC in μg/mL) against bacterial reference strains, haemolytic activity against human RBC (EC_{50} in μg/mL), and toxicity against human HepG2 and MRC-5 cells (EC_{50} in μg/mL).

		Antimicrobial activity (MIC)				Toxicity (EC_{50})			Selectivity index (SI)[a]	
Entry	Mw	*S. aureus*	*C. glutamicum*	*E. coli*	*P. aeruginosa*	RBC	HepG2	MRC-5	RBC/*S. aureus*	RBC/*E. coli*
1a	379.84[b]	>64	16	64	>64	190	>64	–	–	3
1b	415.82[b]	>64	32	>64	>64	208	>64	–	–	–
1c	415.82[b]	>64	>64	>64	>64	–	>64	–	–	–
1d	501.65[b]	16	32	32	>64	211	26	32	13	7
1e	659.44[b]	>64	>64	>64	>64	–	–	–	–	–
1f	479.85[b]	16	8	16	32	89	24	27	6	6
1g	615.85[b]	16	8	32	64	282	20	12	18	9
1h	479.84[b]	32	8	16	64	178	23	18	6	11
1i	479.95[b]	4	2	4	32	>500[f]	12	4	-[f]	-[f]
2a	575.46[c]	>64	>64	>64	>64	–	>64	–	–	–
2b	611.44[c]	>64	64	>64	>64	228	>64	–	–	–
2c	611.44[c]	>64	>64	>64	>64	–	>64	–	–	–
2d	697.27[c]	64	8	64	64	271	48	56	4	4
2e	855.06[c]	2	2	4	4	58	13	17	29	15
2f	675.47[c]	32	8	32	64	312	45	42	10	10
2g	656.34[d]	4	1	4	4	48	11	11	12	12
2h	675.47[c]	8	4	16	32	289	–	16	36	18
2i	675.58[c]	4	2	4	8	74	12	4	19	19
2j	639.60[c]	4	2	16	16	90	–	9	23	6
3d	528.15[d]	16	2	16	16	209	18	8	13	13
3e	841.08[c]	2	1	4	4	24	12	15	12	6
3g	797.49[c]	4	1	4	4	23	7	14	6	6
3i	661.59[c]	2	1	4	4	27	12	9	14	7
4e	939.14[c]	1	0.25	8	4	206	>64	>64	206	26
4g	895.55[c]	2	0.5	4	4	201	>64	>64	101	50
4i	759.66[c]	2	0.5	16	8	329	–	–	165	21
OTC[e]	460.434	0.65	0.65	2.5	20	–	>64	–	–	–

Bacterial reference strains: *Staphylococcus aureus* ATCC 9144; *Corynebacterium glutamicum* ATCC 13032; *Escherichia coli* ATCC 25922, and *Pseudomonas aeruginosa* PA01, DSM 19880 (ATCC 15692).
-: not determined.
[a] Selectivity index (SI) calculated as the RBC EC_{50} value divided by the MIC values against *S. aureus* or *E. coli*.
[b] Mw including 1 equiv. HCl.
[c] Mw including 2 equiv. CF_3COOH as determined by F NMR for **2g**, **3g**, **4g**.
[d] Mw including 2 equiv. HCl.
[e] Reference antibiotic: Oxytetracycline hydrochloride.
[f] Precipitation observed when PBS was added in the RBC assay. The SI was therefore not calculated for **1i**.

(EC_{50}: 18 μg/mL) and MRC-5 (EC_{50}: 8 μg/mL) cell cytotoxicity. Introduction of an additional amino group, and potential increased net positive charge, resulted in increased antimicrobial activity, but a worsening of human cell cytotoxicity.

2.2.4. Reduction of human cell toxicity by diguanylation

Encouraged by the high antimicrobial activities achieved, we were still challenged by the increased human cell toxicity displayed by the triamines **3**. In an effort to reduce human cell toxicity we therefore chose to increase the basicity by guanylating the amino groups of the three most promising diamines **2e**, **2g**, and **2i** to provide the corresponding diguanylated derivatives **4e** (3,5-Br-Ph), **4g** (3,5-CF_3-Ph), and **4i** (4-F-1-Nal) (Scheme 1 and Table 1).

The results for the diguanidines **4** showed a positive effect that introducing two guanidine groups both increased antimicrobial activity and reduced human cell toxicity. The diguanidines **4** were also more potent against Gram-positive bacteria (MIC: 0.25–2 μg/mL) than any of the previous series, and **4e** (3,5-Br-Ph) and **4g** (3,5-CF_3-Ph) showed also good activity against the Gram-negative bacteria (MIC: 4–8 μg/mL). It may be noted that **4i** (4-F-1-Nal) showed reduced potency against the Gram-negative bacteria compared to the corresponding triamine derivative **3i** (4-F-1-Nal). Importantly, derivatives **4e** (3,5-Br-Ph), **4g** (3,5-CF_3-Ph) and **4i** (4-F-1-Nal) were all essentially non-haemolytic (EC_{50}: >200 μg/mL) and displayed no measurable cytotoxicity against human HepG2 and MRC-5 cells within the concentration range tested (EC_{50}: >64 μg/mL). Together, the high antimicrobial activity and lack of toxic effects against human cells resulted in the highest achieved SI values for **4e** (3,5-Br-Ph), **4g** (3,5-CF_3-Ph), and **4i** (4-F-1-Nal). These were in the range of SI: 101–206 with respect to RBC/*S. aureus*, and SI: 21–50 with respect to RBC/*E. coli*.

The reason for the observed lower toxicity of the diguanidines **4** compared with the diamines **2** is not clear. Possible explanations could be: (i) the guanidine derivatives were not able to interact with potential intracellular targets due to decreased diffusion across cell membranes because of higher basicity of guanidine groups (calculated pKa 11.3±0.9) compared to amine groups (calculated pKa 9.3–9.6±0.8), (ii) the diguanidines cause a different cell membrane damaging effect, or (iii) different targets in bacteria and human cells are involved explaining the differences in antimicrobial activity and toxicity. In this respect, the group of Bunker has recently used *in-silico* molecular dynamics simulations to investigate the mechanism of action of previously reported amphipathic α,α-disubstituted β-amino amide derivatives (or $\beta^{2,2}$-amino acid derivatives) [29]. In their studies, they show that the derivatives locate to the lipid-water interface of model membranes, and that the conformation of the lipophilic side-chains differs based on the structure of the hydrophilic groups. The conformation of the lipophilic side-chains also differs depending on interaction with model bacterial or eukaryotic membranes, which can explain variances in antimicrobial efficacy and selectivity.

We have calculated the pKa values *in-silico* of monoamine **1e**, diamine **2e**, triamine **3e**, and diguanidine **4e** to determine the net positive charge at physiological pH 7.4 using the Epik software [33].

In these calculations we also considered how a charged group can alter the pKa of the second amine or guanidine group present in the molecule. The calculations showed that the effect of protonation of a neighbouring group was only relevant for the triamine **3e**, in which the secondary amino group was neutral at pH 7.4 whereas both the primary amino groups were charged. Thus, at physiological pH 7.4 the monoamine **1e** has a net positive charge of +1, while diamine **2e**, triamine **3e**, and diguanidine **4e** all are expected to have a net charge of +2. This was also in accordance with F NMR analysis of the fluorinated series **2g**, **3g**, and **4g** (Supporting information).

A summary of the most important structure-activity relationships (SAR) found for the α,α-disubstituted β-amino amide derivatives is shown in Fig. 2.

2.2.5. Comparison with reference antibiotic

Oxytetracycline hydrochloride was included as reference antibiotic, and displayed MIC values from 0.65 to 2.5 μg/mL against *S. aureus*, *C. glutamicum* and *E. coli*, and a MIC of 20 μg/mL against *P. aeruginosa* (Table 1). These results demonstrated that our most potent derivatives were close to oxytetracycline with respect to antimicrobial activity against the Gram-positive reference strains and *E. coli*.

2.3. Antimicrobial activity against 30 multi-resistant clinical isolates

The most potent derivatives prepared were further screened against 30 multi-resistant clinical isolates of Gram-positive (*S. aureus* and *Enterococcus faecium*) [34–37] and Gram-negative bacteria (*E. coli*, *P. aeruginosa*, *K. pneumoniae*, and *A. baumannii*), including isolates with extended spectrum β-lactamase − carbapenemase (ESBL − CARBA) production and colistin resistance (Table 2). The panel of multi-resistant Gram-negative clinical isolates originated from the strain collection at The Norwegian National Advisory Unit on Detection of Antimicrobial Resistance (K-res) [38–40].

The monoamine derivative **1g** (3,5-CF_3-Ph) was selected based on its favourable activity and advantageous RBC toxicity profile among the monoamines **1**. The results showed that **1g** (3,5-CF_3-Ph) displayed antimicrobial activity against the multi-resistant Gram-positive isolates *S. aureus* and *E. faecium* with MIC values from 8 to 32 μg/mL, but no activity was observed against the multi-resistant Gram-negative clinical isolates within the concentration range tested (up to 32 μg/mL).

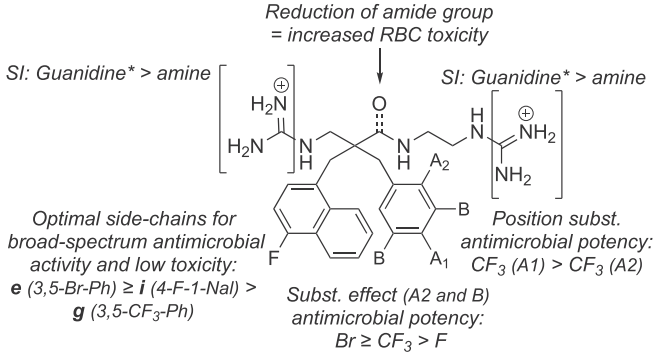

Fig. 2. Summary of SAR for series **2**, **3** and **4** for assuring high antimicrobial activity and low toxicity against human cell lines. Shown in the figure is a hybrid compound − all tested compounds had two identical lipophilic side-chains and were thereby achiral. The effect of side-chain size was also demonstrated by similar antimicrobial potency and toxicity of derivatives with either two 4-F-1-Nal (**2i**, **3i**, **4i**) or two 3,5-CF_3-Ph (**2g**, **3g**, **4g**) side-chains. *Cationic guanidine groups ensured both high antimicrobial activity and low toxicity against RBC, HepG2 and MRC-5 cells.

Five diamine derivatives were tested; **2e** (3,5-Br-Ph), **2f** (2-CF_3-Ph), **2g** (3,5-CF_3-Ph), **2h** (4-CF_3-Ph), and **2i** (4-F-1-Nal). As observed against the bacterial reference strains (Table 1), **2e** (3,5-Br-Ph), **2g** (3,5-CF_3-Ph), and **2i** (4-F-1-Nal) were the overall most potent derivatives and displayed high broad-spectrum activity with MIC values as low as 4–8 μg/mL against individual multi-resistant isolates of *S. aureus*, *E. faecium* and *K. pneumoniae*. The only exception was against *P. aeruginosa* (MIC: ≥32 μg/mL). Derivative **2f** (2-CF_3-Ph) and our reference derivative **2h** (4-CF_3-Ph) were least potent, but MIC values of 8–16 μg/mL were achieved for **2h** (4-CF_3-Ph) against all but one of the Gram-positive *E. faecium* isolates.

High broad-spectrum activity was demonstrated by the triamine derivatives against the multi-resistant clinical isolates. Derivatives **3e** (3,5-Br-Ph), **3g** (3,5-CF_3-Ph), and **3i** (4-F-1-Nal) displayed MIC values of 4–16 μg/mL against multi-resistant *S. aureus*, *E. faecium*, *E. coli*, *K. pneumoniae*, and *A. baumannii*, and MIC values of 16–32 μg/mL against isolates of *P. aeruginosa*. The triamine derivatives were also highly potent against the multi-resistant isolates *K. pneumoniae* K47-25, *K. pneumoniae* 50531633, and *A. baumannii* K63-58, which are resistant to the *last-resort* cationic antibiotic colistin *(Prof. Ørjan Samuelsen, personal communication, K-Res/University Hospital of North Norway - UNN)*. Derivative **3d** (2-Br-Ph) was less potent, but displayed comparable antimicrobial activity as the promising diamine derivatives **2e** (3,5-Br-Ph), **2g** (3,5-CF_3-Ph), and **2i** (4-F-1-Nal).

The optimized diguanidine derivative **4e** (3,5-Br-Ph) showed broad-spectrum antimicrobial activity, and was especially potent against clinical isolates of *S. aureus*, *E. faecium*, and *E. coli* with MIC values of 2–8 μg/mL. Derivative **4e** (3,5-Br-Ph) showed also good activity against individual isolates of *P. aeruginosa* (MIC: 4–8 μg/mL) for all but two exceptions (MIC: 16 μg/mL against *K. pneumoniae* and *A. baumannii*). The diguanidine derivatives **4g** (3,5-CF_3-Ph) and **4i** (4-F-1-Nal) showed acceptable antimicrobial activity against *S. aureus* and *E. faecium*, but were much less potent against the Gram-negative clinical isolates (MIC: 16 ->32 μg/mL). From these studies it could be concluded that the diguanidine derivative **4e** (3,5-Br-Ph) was a highly potent lead compound against multi-resistant clinical isolates of Gram-positive and Gram-negative bacteria, and also favourably with respect to human cell line toxicity.

2.4. Phase I metabolism

Introduction of fluorine-atoms into chemical scaffolds is a common strategy in drug development to prevent hepatic CYP450 Phase I oxidation of aromatic groups [41]. As we have reported previously, α,α-disubstituted β-amino amides are susceptible to Phase I oxidations, especially derivatives having electron rich (2-naphthyl)methyl side chains [30]. This study revealed extensive metabolism, in which the main metabolites are hydroxylation of the aromatic (2-naphthyl)methyl side-chains. For α,α-disubstituted β-amino amides with 4-*tert*-butylbenzyl side chains the *tert*-butyl group is oxidised, whereas the side chain of our previously reported halogenated **2h** (4-CF_3-Ph) is inert to Phase I oxidation [6,30]. Hepatic CYP450 enzymes are membrane-associated and metabolise preferably lipophilic substrates and to a minor extent hydrophilic substrates. To further investigate the effect of halogenated substituents on metabolic stability, three representatives of halogenated diamine derivatives **2e** (3,5-Br-Ph), **2g** (3,5-CF_3-Ph), and **2i** (4-F-1-Nal) were selected for Phase 1 metabolism studies using murine liver microsomes. The diamine derivatives were preferred for side chain metabolism studies in place of the more hydrophilic diguanidines **4**.

The results confirmed our expectations for the halogenated

Table 2
Antimicrobial activity (MIC in μg/mL) of the most potent derivatives against 30 multi-resistant clinical isolates.

Multi-resistant isolates	1g	2e	2f	2g	2 h	2i	3d	3e	3g	3i	4e	4g	4i	ESBL-CARBA[a]
S. aureus N315	>32	8	>32	16	>32	16	8	4	8	4	2	4	4	
S. aureus NCTC 10442	32	8	>32	16	>32	8	16	4	8	4	2	8	4	
S. aureus strain 85/2082	32	8	>32	16	>32	8	8	8	8	4	2	8	4	
S. aureus strain WIS	16	16	>32	16	>32	16	8	8	8	4	2	8	4	
S. aureus IHT 99040	16	16	32	8	>32	16	8	8	8	8	2	8	4[b]	
E. faecium 50673722	16	8	32	8	16	16	16	4	4	4	4	8[b]	16	
E. faecium 50901530	16	8	32	4	16	16	16	4	8	4	4	4[b]	4[b]	
E. faecium K36-18	8	8	>32	8	16	16	16	8	8	4	4	8[b]	16	
E. faecium 50758899	8	8	>32	4	32	8	16	4	8	4	4	8[b]	16	
E. faecium TUH50-22	8	8	>32	8	8	8	16	4	4	4	2	4	8[b]	
E. coli 50579417	>32	8	>32	16	>32	8	16	16	8	8	8[b]	32[b]	32	OXA-48
E. coli 50639799	>32	16	>32	16	>32	16	16	8	8	8	8[b]	16[b]	32	VIM-29
E. coli 50676002	>32	16	>32	16	>32	8	16	8	8	8	8[b]	32[b]	32[b]	NDM-1
E. coli 50739822	>32	8	>32	16	32	16	16	8	8	4	8[b]	32[b]	32[b]	NDM-1
E. coli 50857972	>32	8	>32	8	32	8	16	8	8	8	8[b]	32[b]	32	IMP-26
P. aeruginosa K34-7	>32	>32	>32	>32	>32	>32	32	16	32	16	16[b]	32	>32	VIM-2
P. aeruginosa K34-73	>32	32	>32	32	>32	32	32	16	32	16	16	16	>32	VIM-4
P. aeruginosa K44-24	>32	32	>32	>32	>32	32	32	16	32	16	16	32	>32	IMP-14
P. aeruginosa 50692172	>32	>32	>32	32	>32	>32	32	32	16	16	8[b]	32[b]	>32	NDM-1
P. aeruginosa 50692520	>32	>32	>32	>32	>32	>32	16	32	32	16	4	16	>32	VIM
K. pneumoniae K47-25[c]	>32	16	>32	32	>32	32	16	8	16	8	32[b]	>32	>32	KPC-2
K. pneumoniae K66-45	>32	32	>32	32	>32	8	16	8	8	8	16[b]	>32	>32	NDM-1
K. pneumoniae 50531633[c]	>32	16	>32	16	32	8	16	8	8	4	16	>32	>32	NDM-1 +OXA-181
K. pneumoniae 50625602	>32	8	>32	16	32	8	16	16	8	8	16[b]	>32	>32	OXA-245
K. pneumoniae 50667959	>32	16	>32	16	32	8	16	16	8	8	16	>32	>32	VIM-1
A. baumannii K12-21	>32	32	>32	8	>32	32	16	16	8	8	16[b]	>32	>32	OXA-58
A. baumannii K44-35	>32	32	>32	16	>32	>32	16	8	8	8	16[b]	>32	>32	OXA-23
A. baumannii K47-42	>32	16	>32	16	>32	16	16	16	8	16	16[b]	>32	>32	OXA-23
A. baumannii K55-13	>32	16	>32	16	>32	32	16	8	8	16	16[b]	>32	>32	OXA-24
A. baumannii K63-58[c]	>32	32	>32	8	>32	16	16	8	8	8	16[b]	>32	>32	OXA-23

[a] ESBL-CARBA: Extended spectrum β-lactamase − carbapenemase producing isolates. OXA, oxacillinase; VIM, Verona integron-encoded metallo-β-lactamase; NDM, New Delhi metallo-β-lactamase; IMP, imipenem-type carbapenemase; KPC, *K. pneumoniae* carbapenemase.
[b] Precipitation observed as described in the methods section.
[c] Clinical isolates resistant to the antibiotic colistin.

derivatives **2e** (3,5-Br-Ph) and **2g** (3,5-CF_3-Ph), in which reversed-phase high-performance liquid chromatography - mass spectrometry (RP-HPLC-MS) analysis was unable to detect formation of any metabolites resulting from, e.g., deamination, oxidation (hydroxylation), or dioxidation (dihydroxylation) for up to 3 h of incubation (results not presented). For the (4-fluoronapht-1-yl)methyl derivative **2i** (4-F-1-Nal) approx. 9% was metabolised after 3 h of incubation (Fig. 3). Three different Phase I oxidised metabolites were detected from **2i** (4-F-1-Nal) as shown in Scheme 2. The main metabolite resulted from hydroxylation of one of the side-chains in **2i** (4-F-1-Nal) counting for approx. 7% of the total amount of metabolites formed after 3 h. We were not able to determine the exact

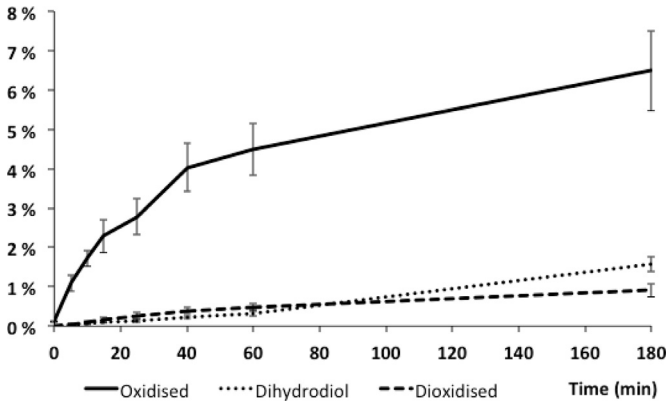

Fig. 3. Formation of Phase I metabolites from **2i** (4-F-1-Nal) over time by oxidation in murine liver microsomes (y-axis: percentage of formed metabolites from **2i**).

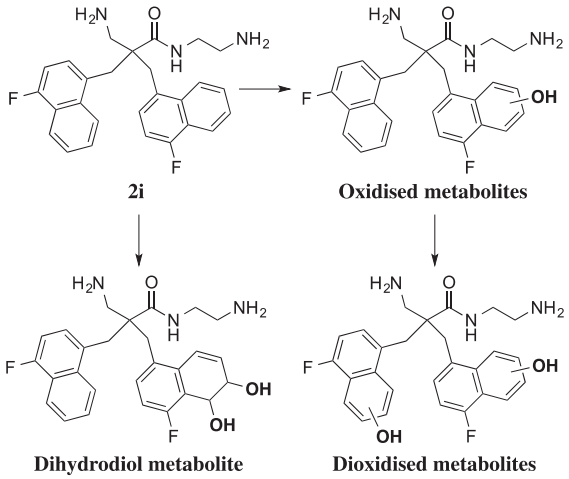

Scheme 2. Phase I metabolites formed from **2i** (4-F-1-Nal) by oxidation in murine liver microsomes. Dioxidised metabolites (lower; right) may involve dioxidation on one of the **2i** (4-F-1-Nal) side-chains or oxidation on both side-chains.

position of oxidation, but a total of four different isomeric metabolites were detected, as observed by RP-HPLC-MS analysis. The analysis also revealed small amounts of a dihydrodiol metabolite, and four different dioxidised metabolites with varying retention times (Scheme 2). However, due to the low abundance of the dioxidised metabolites, we were unable to distinguish between dioxidation on one of the **2i** (4-F-1-Nal) side chains from oxidation of both side chains.

Based on these results, it was evident that the halogenated

substituents on the side chains of the α,α-disubstituted β-amino amides provided protection against Phase I oxidations for **2e** (3,5-Br-Ph) and **2g** (3,5-CF_3-Ph), and also substantially lowered the formation of Phase I metabolites from **2i** (4-F-1-Nal) compared to previously reported derivatives with (2-naphthyl)methyl side-chains [30]. Based on the presumed membrane disrupting mechanism of action, oxidation of the aromatic side chains is likely to result in metabolites with reduced antimicrobial potency because of reduced overall lipophilicity. This is supported by the low potency of a previously reported α,α-disubstituted β-amino amide derivative with 3,5-dimethoxy benzylic side-chains [8].

3. Conclusions

Design of small amphipathic peptidomimetics is an attractive strategy for developing novel antimicrobial agents resembling the unique mode of action of larger AMPs that disrupt bacterial membranes. Inspired by nature, synthesis of small peptidomimetics offer great possibilities for developing new compounds with high antimicrobial activity and favourable pharmacokinetic properties (ADMETox), such as improved proteolytic stability and tolerable toxicity. We have through a systematic study and screening against bacterial reference strains and 30 multi-resistant clinical isolates shown that halogenated α,α-disubstituted β-amino amides, amines and guanidines are promising antimicrobial agents, also against challenging Gram-negative multi-resistant clinical isolates. The diguanidine derivative **4e** (3,5-Br-Ph) showed exceptional high antimicrobial activity against both bacterial reference strains and multi-resistant clinical isolates, and no major *in vitro* human cell toxicity. Studies with liver microsomes also showed that the lipophilic side-chains of **4e** (3,5-Br-Ph) were not susceptible for Phase I oxidations and may thereby provide high metabolic stability *in vivo*. The study has surveyed in total nine different halogenated aromatic side-chains that can have beneficial effects also in other antimicrobial peptidomimetics and AMPs as lipophilic constituents. Especially the halogenated lipophilic groups **e** (3,5-Br-Ph), **g** (3,5-CF_3-Ph), and **i** (4-F-1-Nal) (Scheme 1) may be worth implementing in SAR studies to improve antimicrobial potency, modify human cell toxicity, and improve pharmacokinetic properties such as *in vivo* stability.

4. Experimental section

4.1. Chemicals and equipment

All reagents and solvents were purchased from commercial sources and used as supplied unless otherwise stated. Anhydrous THF was prepared by storage over 4 Å molecular sieves. Raney-Nickel was bought from Sigma Aldrich (CAS no. 7440-02-0, 2800, slurry, in H_2O, active catalyst). Reactions were monitored by thin-layer chromatography (TLC) with Merck pre-coated silica gel plates (60 F_{254}). Visualization was accomplished with either UV light or by immersion in potassium permanganate or phosphomolybdic acid (PMA) followed by light heating with a heating gun. Purification of reactions was carried out by chromatography using a reversed-phase (RP) C_{18} column preloaded on a Samplet® cartridge belonging to a Biotage SP-1 system. Analytical RP-HPLC was carried out on a Waters 2695 Separations Module equipped with an XBridge™ C_{18} 5 μm, 4.6 mm × 250 mm column and analysed at wavelengths 214 and 254 nm with a Waters 996 PDA detector spanning from wavelengths 210–310 nm. The derivatives were eluted with a mobile phase consisting of water and acetonitrile, both containing 0.1% TFA. The gradient started at 10% acetonitrile (3 min), followed by a linear gradient to 90% acetonitrile over 17 min. The flow rate was 1 mL min^{-1}. NMR spectra were obtained on both a 400 MHz Bruker Avance III HD equipped with a 5 mm SmartProbe BB/1H (BB = 19F, 31P–15 N) and a 600 MHz Varian Inova spectrometer (Agilent, St. Clara, CA, USA) equipped with an inverse HCN probe with cryogenic enhancement for 1H. Data are represented as follows: chemical shift, multiplicity (s = singlet, d = doublet, t = triplet, q = quartet, p = pentet, h = heptett, m = multiplet), coupling constant (*J*, Hz) and integration. Chemical shifts (δ) are reported in ppm relative to the residual solvent peak ($CDCl_3$: δ_H 7.26, and δ_C 77.16; Methanol-d_4: δ_H 3.31 and δ_C 49.00, DMSO-d_6: δ_H 2.50 and δ_C 39.52). Positive ion electrospray ionization mass spectrometry (ESI-MS) was conducted on a Thermo electron LTQ Orbitrap XL spectrometer with an Electrospray ion source (ION-MAX) - Thermo scientific.

4.2. Synthesis of test derivatives

Synthesis and spectroscopic data for derivatives **5a-h**, **1a-h**, and **2a-h** have previously been published by our group [32]. Compounds **1a**–**i** were evaluated as HCl salts obtained from treatment with HCl in ether. All compounds tested were >95% pure as determined by analytical HPLC, with exception of **2j** which was 85% pure. *1-(Bromomethyl)-4-fluoronaphthalene* was synthesized according to literature procedures from 4-fluoro-1-naphthoic acid [42].

Preparation of $ZnCl_2$/$NaBH_4$ reducing agents. The reducing agent was prepared by stirring $ZnCl_2$ (1 equiv., 1.15 g) and $NaBH_4$ (2 equiv., 0.68 g) in dry THF (40 mL) overnight.

Methyl 2-cyano-3-(4-fluoro-1-naphthyl)-2-[(4-fluoro-1-naphthyl)methyl]propionate (**5i**). Methyl 2-cyanoacetate (8.53 mmol, 0.753 mL) was dissolved in CH_2Cl_2 (40 mL, prefiltered through K_2CO_3), cooled to 0 °C, added DBU (2.62 mL, 2.00 equiv.), and stirred for 2 min. 1-(Bromomethyl)-4-fluoronaphthalene (4.20 g, 2.05 equiv.) was added in small portions to avoid increase in temperature. The reaction was left to stir at r.t. until completion was indicated by TLC (1:4 EtOAc/toluene). After completion, the reaction was quenched with water and extracted with EtOAc. The organic phase was washed with water (3 times) and brine, dried over Na_2SO_4, filtered and evaporated to dryness. To remove residual EtOAc, chloroform was added and re-evaporated. MeOH was added to precipitate the crude. The resulting solid was recrystallized in MeOH to give the title derivative (**5i**) as light brown crystals (3.41 g, 96%). ^{1}H NMR (400 MHz, $CDCl_3$) δ 8.16 (d, J = 7.9 Hz, 2H), 8.06 (d, J = 8.3 Hz, 2H), 7.71–7.53 (m, 4H), 7.49 (dd, J = 8.0, 5.4 Hz, 2H), 7.14 (dd, J = 10.0, 8.0 Hz, 2H), 3.86 (d_{AB}, J = 14.4 Hz, 2H), 3.70 (d_{AB}, J = 14.4 Hz, 2H), 3.37 (s, 3H). ^{13}C NMR (101 MHz, $CDCl_3$) δ 169.0, 158.6 (d, J = 253.0 Hz), 133.4 (d, J = 4.5 Hz), 128.4 (d, J = 8.6 Hz), 127.1, 126.2 (d, J = 4.6 Hz), 126.1 (d, J = 1.9 Hz), 123.9 (d, J = 15.9 Hz), 123.7 (d, J = 2.6 Hz), 121.1 (d, J = 6.0 Hz), 118.6, 108.9 (d, J = 20.2 Hz), 53.4, 52.5, 38.3. HRMS-ESI *m/z*: $C_{26}H_{19}F_2KNO_2$ $[M+K]^+$ calculated for 454.1013, found: 454.1020.

3-(2-Aminoethylamino)-2,2-bis[(4-fluoro-1-naphthyl)methyl]-3-oxopropiononitrile (**1i**). The reaction was performed under N_2. Methyl 2-cyano-3-(4-fluoro-1-naphthyl)-2-[(4-fluoro-1-naphthyl) methyl]propionate (**5i**) (6.97 mmol, 2.89 g) was added ethylenediamine (20 mL) and stirred at room temperature for 24 h and completion was indicated by TLC (1:4 EtOAc/toluene). After completion, the reaction mixture was cooled on ice and water was added to the reaction mixture until precipitation occurred. The product was filtered off, washed carefully with water and dried under vacuum to give the title derivative (**1i**) as light brown powder (2.47 g, 80%). ^{1}H NMR (400 MHz, Methanol-d_4) δ 8.31 (dt, J = 8.1, 1.7 Hz, 2H), 8.10 (dd, J = 8.0, 1.6 Hz, 2H), 7.71–7.46 (m, 6H), 7.16 (dd, J = 10.4, 8.0 Hz, 2H), 3.97 (d_{AB}, J = 14.2 Hz, 2H), 3.83 (d_{AB}, J = 14.2 Hz, 2H), 2.87 (t, J = 6.5 Hz, 2H), 2.22 (t, J = 6.5 Hz, 2H). ^{13}C NMR (101 MHz, $CDCl_3$) δ 166.7, 158.8 (d, J = 252.9 Hz), 133.8 (d,

$J = 4.5$ Hz), 128.9 (d, $J = 8.6$ Hz), 127.3, 127.1 (d, $J = 4.6$ Hz), 126.4 (d, $J = 1.9$ Hz), 124.4 (d, $J = 2.7$ Hz), 124.1 (d, $J = 15.9$ Hz), 121.3 (d, $J = 6.0$ Hz), 120.6, 109.1 (d, $J = 20.1$ Hz), 53.6, 42.9, 40.1, 38.2. HRMS-ESI: $C_{27}H_{24}F_2N_3O$ $[M+H]^+$ calculated for 444.1882, found: 444.1883.

3-Amino-1-(2-aminoethylamino)-2,2-bis[(4-fluoro-1-naphthyl) methyl]-1-propanone (**2i**). The nitrile **1i** (0.11 mmol, 0.050 g, 1 equiv.) was dissolved in $ZnCl_2/NaBH_4$ reducing agent (1 mL) and refluxed for 1.5 h. The reaction mixture was allowed to cool down to r.t., quenched with water (0.1 mL) followed by 6 M aqueous HCl (1 mL). A complex of a boron and **2i** was detected by MS, which dissociated on reflux of the mixture for 10 min (followed by MS). The resulting solution was evaporated to dryness, the residue dissolved in MeOH and purified by C_{18} RP flash chromatography and lyophilized to give the title derivative (**2i**) as light brown powder (0.038 g, 45%, TFA salt). ^{1}H NMR (400 MHz, Methanol-d_4) δ 8.17 (dd, $J = 18.3$, 8.2 Hz, 4H), 7.64 (dt, $J = 15.1$, 7.0 Hz, 4H), 7.56–7.31 (m, 2H), 7.29–7.00 (m, 2H), 3.75 (d_{AB}, $J = 15.1$ Hz, 2H), 3.68 (d_{AB}, $J = 15.1$ Hz, 2H), 3.24 (t, $J = 6.4$ Hz, 2H), 3.13 (s, 2H), 2.86 (t, $J = 6.4$ Hz, 2H). ^{13}C NMR (101 MHz, Methanol-d_4) δ 176.7, 159.5 (d, $J = 250.9$ Hz), 135.6 (d, $J = 4.2$ Hz), 129.4 (d, $J = 8.5$ Hz), 129.0 (d, $J = 4.4$ Hz), 128.5, 127.3 (d, $J = 1.9$ Hz), 125.5 (d, $J = 2.6$ Hz), 125.2 (d, $J = 15.9$ Hz), 121.9 (d, $J = 6.1$ Hz), 109.8 (d, $J = 20.2$ Hz), 51.6, 44.3, 40.4, 38.7, 36.9. m/z: $C_{27}H_{28}F_2N_3O$ $[M+H]^+$ calculated for 448.2195, found: 448.2194.

3-*Amino-1-(2-aminoethylamino)-2,2-bis[(1-naphthyl)methyl]-1-propanone* (**2j**). One spoon of Raney-Nickel (approx. 5 g) was transferred to a round bottomed flask, washed with MeOH (3 × 15 mL) and EtOAc (3 × 15 mL) before addition of compound **1i** (0.114 g, 0.25 mmol) dissolved in EtOAc. Boc_2O (0.224 g, 1.03 mmol, 4 equiv.) was added. The reaction was stirred for 18 h at 45 °C with a H_2(g) containing balloon attached. The reaction mixture was cooled to r.t. before the catalyst was filtered off through a pad of sand and celite under N_2, washed with brine, dried with Na_2SO_4, and evaporated to dryness. The Boc-protected intermediate was added dioxane (4 mL), H_2O (0.5 mL), and 4 M HCl/dioxane (2 mL) to yield the crude HCl-salt. The product was purified by C_{18} RP flash chromatography. ^{1}H NMR (400 MHz, Methanol-d_4) δ 7.90–7.82 (m, 6H), 7.75 (d, $J = 1.7$ Hz, 2H), 7.56–7.46 (m, 4H), 7.38 (dd, $J = 8.4$, 1.8 Hz, 2H), 3.53 (t, $J = 6.5$ Hz, 2H), 3.42 (d, $J = 14.2$ Hz, 2H), 3.20 (d, $J = 14.1$ Hz, 2H), 3.12–3.08 (m, 4H). ^{13}C NMR (101 MHz, Methanol-d_4) δ 177.1, 134.8, 134.1, 134.0, 130.4, 129.4, 129.3, 128.7, 128.7, 127.5, 127.2, 51.0, 43.8, 41.4, 40.6, 38.7. HRMS-ESI *m/z*: $C_{27}H_{30}N_3O$ $[M+H]^+$ calculated for 412.2382, found: 412.2394.

Preparation of triamine derivatives ***3***. Derivatives **3d**, **3e**, **3g**, and **3i** were prepared in accordance to the procedure for nitrile reduction of **2i** with $ZnCl_2/NaBH_4$, but with 24 h reaction time [32].

3-Amino-1-(2-aminoethylamino)-2,2-bis[(o-bromophenyl) methyl]propane (**3d**). The nitrile **1d** (0.985 mmol, 0.455 g) and the $ZnCl_2/NaBH_4$ reducing agent (7.0 mL) gave the title derivative (**3d**) as clear crystals (HCl-salt) after purification by C_{18} RP flash chromatography with acetonitrile/water and lyophilized with aq. HCl (0.123 g, 22%). ^{1}H NMR (600 MHz, DMSO-d_6) δ 10.04 (s, 2H), 8.66 (s, 3H), 8.44 (s, 3H), 7.66 (d, $J = 8.1$ Hz, 2H), 7.51 (d, $J = 7.6$ Hz, 2H), 7.43 (t, $J = 7.6$ Hz, 2H), 7.26 (t, $J = 7.8$ Hz, 2H), 3.39 (s*, 2H), 3.36(s*, 2H), 3.31 (d*, $J = 14.6$ Hz, 2H), 3.25 (d*, $J = 14.9$ Hz, 2H), 2,97 (s*, 2H), 2.91 (s*, 2H). * Extensive line broadening due to conformational exchange. ^{13}C NMR (151 MHz, DMSO-d_6) δ 134.8, 133.3, 133.0, 129.4, 128.0, 125.9, 50.2, 46.3, 42.4, 41.3, 36.2, 35.2. HRMS-ESI *m/z*: $C_{19}H_{26}^{79}Br_2N_3$ $[M+H]^+$ calculated for 454.0486, found: 454.0495.

3-Amino-1-(2-aminoethylamino)-2,2-bis[(3,5-dibromophenyl) methyl]propane (**3e**). The nitrile **1e** (0.33 mmol, 0.205 g) and the reducing agent (3.0 mL) gave the title derivative (**3e**) as clear crystals after purification (TFA-salt) (0.068 g, 22%). ^{1}H NMR (400 MHz, Methanol-d_4) δ 7.69 (s, 2H), 7.44 (s, 4H), 3.15 (t, $J = 6.4$ Hz, 2H), 3.06 (s, 2H), 2.96 (t, $J = 6.4$ Hz, 2H), 2.88–2.68 (m, 6H). ^{13}C NMR (101 MHz, Methanol-d_4) δ 141.4, 134.0, 133.7, 124.1, 55.6, 48.3, 46.8, 40.8, 40.5, 39.7. HRMS-ESI *m/z*: $C_{19}H_{24}^{79}Br_4N_3$ $[M+H]^+$ calculated for 609.8694, found: 609.8719.

3-Amino-1-(2-aminoethylamino)-2,2-bis([3,5-bis(trifluoromethyl)phenyl]methyl) propane (**3g**). The nitrile **1g** (0.18 mmol, 0.104 g) and the reducing agent (2.7 mL) gave the title derivative (**3g**) as clear crystals after purification (TFA-salt) (0.061 g, 37%). ^{1}H NMR (400 MHz, Methanol-d_4) δ ^{1}H NMR (400 MHz, Methanol-d_4) δ 7.92 (s, 2H), 7.88 (s, 4H), 3.10 (s, 4H), 3.04 (d_{AB}, $J = 13.8$ Hz, 2H), 2.93 (d_{AB}, $J = 13.6$ Hz, 2H), 2.87 (t, $J = 6.0$ Hz, 2H), 2.74 (s, 2H). ^{13}C NMR (101 MHz, Methanol-d_4) δ 140.3, 132.9 (q, $J = 33.1$ Hz), 132.37–132.14 (m), 124.8 (q, $J = 272.0$ Hz), 122.2 (h, $J = 3.7$ Hz), 55.9, 48.3 (overlap with solvent, confirmed by HSQC), 47.2, 40.8, 40.7, 40.0. HRMS-ESI *m/z*: $C_{23}H_{24}F_{12}N_3$ $[M+H]^+$ calculated for 570.1774, found: 570.1766.

3-Amino-1-(2-aminoethylamino)-2,2-bis[(4-fluoro-1-naphthyl) methyl]propane (**3i**). The nitrile **1i** (0.33 mmol, 0.145 g) and the reducing agent (3.0 mL) gave the title derivative (**3i**) as clear crystals (TFA-salt) after purification (0.093 g, 36%). ^{1}H NMR (400 MHz, Methanol-d_4) δ 8.14 (dt, $J = 6.3$, 2.7 Hz, 2H), 8.05–7.89 (m, 2H), 7.58 (dd, $J = 6.5$, 3.1 Hz, 4H), 7.40 (t, $J = 6.7$ Hz, 2H), 7.23 (td, $J = 9.2$, 8.0, 2.3 Hz, 2H), 3.47–3.25 (m, 10H), 3.20 (s, 2H), 3.04 (t, $J = 5.9$ Hz, 2H), 2.93 (s, 2H), 2.84 (t, $J = 5.6$ Hz, 2H). ^{13}C NMR (101 MHz, Methanol-d_4) δ 159.5 (d, $J = 251.1$ Hz), 135.8 (d, $J = 4.2$ Hz), 129.8 (d, $J = 8.4$ Hz), 129.6 (d, $J = 4.8$ Hz), 128.5, 127.4 (d, $J = 1.9$ Hz), 125.47–125.20 (m), 125.4 (d, $J = 2.8$ Hz), 122.1 (d, $J = 6.2$ Hz), 109.9 (d, $J = 20.1$ Hz), 56.5, 48.3, 47.7, 42.9, 39.8, 36.3. HRMS-ESI *m/z*: $C_{27}H_{30}F_2N_3$ $[M+H]^+$ calculated for 434.2402, found: 434.2420.

Preparation of guanidine derivatives ***4***. Derivatives **4e**, **4g**, and **4i** were prepared using the following procedure: To a stirred solution of the salt of **2e** (HCl), **2g** (HCl) or **2i** (TFA) in THF, K_2CO_3 was added followed by *N,N′*-Di-Boc-1H-pyrazole-1-carboxamidine. The reaction was stirred at r.t. for 48–72 h. The reaction mixture was concentrated, the crude product was dissolved in EtOAc and washed with water and brine. The organic phase was dried over Na_2SO_4, filtered and concentrated. The crude product was purified by automated flash chromatography (EtOAc/Heptane) and the resulting Boc-protected intermediate was deprotected with TFA (1 mL) in CH_2Cl_2 (1:1) for 18 h. The reaction mixture was concentrated and the crude was purified by RP automated flash chromatography (ACN/water 0,1% TFA) and lyophilized to yield the guanylated product.

2,2-bis(3,5-dibromobenzyl)-3-guanidino-N-(2-guanidinoethyl) propenamide **(4e)**. The HCl salt of **2e** (120 mg, 0.17 mmol, 1 equiv.) was dissolved in THF (5 mL) and added K_2CO_3 (118 mg, 0.85 mmol, 5 equiv.) and *N,N′*-Di-Boc-1H-pyrazole-1-carboxamidine (221 mg, 4 equiv.) and stirred for 72 h. The reaction mixture was then treated according to the general procedure to yield the title compound **4e** as a white powder (TFA-salt, 55 mg, 34%). ^{1}H NMR (400 MHz, Methanol-d_4) δ 7.67 (t, $J = 1.7$ Hz, 2H), 7.32 (d, $J = 1.7$ Hz, 4H), 3.45–3.39 (m, 2H), 3.37–3.32 (m, 2H), 3.21 (d_{AB}, $J = 14.0$ Hz, 2H), 3.10 (s, 2H), 2.91 (d_{AB} $J = 14.1$ Hz, 2H). ^{13}C NMR (101 MHz, Methanol-d_4) δ 175.6, 158.9, 158.9, 141.4, 134.0, 133.0, 124.0, 52.6, 43.8, 42.1, 41.3, 40.1. HRMS-ESI *m/z*: $[M+H]^+$ calculated for $C_{21}H_{26}^{79}Br_4N_7O^+$ 707.8926, found: 707.8947.

2,2-bis(3,5-bis(trifluoromethyl)benzyl)-3-guanidino-N-(2-guanidinoethyl)propenamide **(4g)**. The HCl salt of **2g** (34 mg, 0.052 mmol, 1 equiv.) was dissolved in THF (3 mL) and added K_2CO_3 (35 mg, 0.25 mmol, 5 equiv.) and *N,N′*-Di-Boc-1H-pyrazole-1-carboxamidine (66 mg, 0.21 mmol, 4 equiv.) and stirred for 72 h. The reaction mixture was then treated according to the general procedure to yield the title compound **4e** as a white powder (TFA-salt, 17 mg, 37%). ^{1}H NMR (400 MHz, Methanol-d_4) δ 7.91 (s, 2H), 7.75 (s, 4H), 3.49 (d_{AB}, $J = 14.2$ Hz, 2H), 3.41–3.35 (m, 2H), 3.34–3.32 (m, 2H), 3.19 (d_{AB}, $J = 14.2$ Hz, 2H), 3.08 (s, 2H). ^{13}C NMR (101 MHz, Methanol-d_4) δ 175.0, 162.9 (q, $J = 35.6$ Hz, TFA), 159.1,

158.9, 140.2, 132.9 (q, $J = 33.2$ Hz), 131.6–131.4 (m), 124.7 (q, $J = 272.0$ Hz), 122.5–122.2 (m), 118.0 (q, $J = 292.0$ Hz, TFA), 52.7, 43.8, 41.6, 41.3, 40.1, 31.7. HRMS-ESI *m/z*: $[M+H]^+$ calculated for $C_{25}H_{26}F_{12}N_7O^+$ 688.2003, found: 668.2005.

3-(4-fluoronaphthalen-1-yl*)-2-((4-fluoronaphthalen*-1-yl*) methyl)-N-(2-guanidinoethyl)-2-(guanidinomethyl)propenamide* **(4i).**The TFA salt of **2i** (25 mg, 0.037 mmol, 1 equiv.) was dissolved in THF (2 mL) and added K_2CO_3 (20 mg, 0.14 mmol, 4 equiv.) and *N,N′*-Di-Boc-1H-pyrazole-1-carboxamidine (32 mg and an extra 15 mg after 24 h, 0.15 mmol, 4 equiv.). The reaction mixture was then treated according to the general procedure to yield the title compound **4i** as a light brown powder (TFA-salt, 13 mg, 46%). ^{1}H NMR (400 MHz, Methanol-d_4) δ 8.22–8.17 (m, 2H), 8.12 (dd, $J = 8.1$, 1.7 Hz, 2H), 7.66–7.56 (m, 4H), 7.35 (dd, $J = 8.1$, 5.4 Hz, 2H), 7.15 (dd, $J = 10.3$, 8.0 Hz, 2H), 3.71 (d_{AB}, $J = 15.2$ Hz, 2H), 3.62 (d_{AB}, $J = 15.2$ Hz, 2H), 3.36 (s, 2H), 3.07 (t, $J = 6.4$ Hz, 2H), 2.94 (t, $J = 6.4$ Hz, 2H). ^{13}C NMR (101 MHz, Methanol-d_4) δ 176.8, 159.4 (d, $J = 250.8$ Hz), 158.8, 158.7, 135.5 (d, $J = 4.2$ Hz), 129.6 (d, $J = 4.7$ Hz), 128.9 (d, $J = 8.4$ Hz), 128.3, 127.3 (d, $J = 1.9$ Hz), 125.6–124.8 (m), 121.9 (d, $J = 6.2$ Hz), 109.7 (d, $J = 20.0$ Hz), 52.6, 45.6, 41.6, 39.9, 37.7. HRMS-ESI *m/z*: $[M+H]^+$ calculated for $C_{29}H_{32}F_2N_7O_2^+$ 532.2631, found: 532.2631.

4.3. Biological test methods

Minimum inhibitory concentration (MIC) assay: Stock solutions of the test derivatives were prepared with up to 100% DMSO and stored at −20 °C. If necessary, the solutions were heated to 40–80 °C before testing to facilitate complete dissolution. Double-distilled water was used in all dilutions prepared. The final concentration of DMSO in the test series was ≤1% and did not affect the assay results. A microdilution susceptibility test was used for MIC determination according to CLSI M07-A9 [43] with modifications as described by Igumnova et al. [44]. Briefly, the bacterial inoculum was adjusted to approximately 2.5–3 x 10^4 cells/mL in Mueller-Hinton broth (MHB, Difco Laboratories, USA), and incubated in a ratio of 1:1 with test derivatives in polystyrene 96-well flat-bottom microplates (NUNC, Roskilde, Denmark). Positive growth control (without test derivatives) and negative control (without bacteria) were included. The reference antibiotic was oxytetracycline hydrochloride (Sigma Aldrich, Saint Louis, MO, USA). The microplates were placed in an incubator set to 37 °C (20 °C for *C. glutamicum*) for 24 h. The MIC value was defined as the lowest concentration of derivative resulting in no bacterial growth as determined by OD_{600} measurement using a Synergy H1 Hybrid Multi-Mode micro plate reader (BioTek Instruments Inc., Winooski, VT, USA). All derivatives were tested in three parallels.

Antimicrobial screening against clinical isolates: The Norwegian National Advisory Unit on Detection of Antimicrobial Resistance (K-res), University Hospital of Northern-Norway (UNN), provided the collection of 30 multi-drug resistant isolates in Table 2. The MIC was determined as explained above with some exceptions; working solutions of test derivatives were prepared from concentrated DMSO stocks stored at r.t., the density of the bacterial inoculum was increased 40 x to 1–1.2 × 10^6 cells/mL, enterococci were incubated in Brain Heart Infusion broth (BHIB, Difco Laboratories, USA), the microplates were incubated for 24 h, and the derivatives were tested in four parallels. Also, in this assay, optical density (OD) is proportional to the amount of bacteria and should be equal to the OD of the control when bacterial growth is completely inhibited. However, for some compounds the OD was not reduced to the control level even though complete inhibition was expected due to the stepwise increase in concentration. The remaining OD might be explained by precipitation of compounds and media components, residues of bacterial culture, etc. Thus, the term "inhibitory concentration" (IC) is used to define the point where a major decrease of OD is observed. The IC should reflect the impact of tested compounds on bacteria and correlate with the MIC.

Determination of haemolytic activity: The protocol was adapted from Tørfoss et al. [45]. In brief, a heparinizied fraction (10 USP units/mL) human blood was used for haemolysis determination whereas a second fraction in test tubes containing EDTA (Vacutest®, KIMA, Arzergrande, Italy) was used for determination of the hematocrit (hct). Plasma was removed from the heparinized blood by washing three times with pre-warmed PBS before adjustment to 10% hct. Stock solutions of derivatives in DMSO were dissolved in PBS with a final DMSO content ≤1%. The positive control for 100% haemolysis consisted of 1% Triton X-100 (Sigma-Aldrich). A negative control containing 1% DMSO in PBS buffer was included and no signs of toxicity were detected. Test solutions and erythrocytes (1% v/v final concentration) were mixed and incubated under agitation at 37 °C for 1 h. After centrifugation, 100 μL of each reaction vial were transferred to a 96-well plate in triplicate and diluted with PBS if necessary. Absorbance was recorded with a microplate reader (VersaMax™, Molecular Devices, Sunnyvale, CA, USA), at 405 nm and 545 nm. After subtracting PBS background, the percentage of haemolysis was calculated as the ratio of the absorbance in the derivative-treated and surfactant-treated samples. Experiments were performed in three independent replicates and EC_{50} values are reported as an average.

Determination of cytotoxicity: Cytotoxicity was studied using HepG2 cells (human liver carcinoma) and MRC-5 cells (human lung fibroblasts). The cells were seeded at 35 000 and 15 000 cells per well respectively. The cells were incubated at 37 °C, 5% CO_2 overnight. Test compounds diluted in MEM Earle's without FBS were added to the cells and incubated for 4 h. After incubation, 10 μL of CellTiter 96® AQueous One Solution Reagent (Promega, Madison, WI, USA) was added and the plates were then incubated further for 1 h. Absorbance was measured at 485 nm using a DTX 880 Multimode Detector. Results were calculated as % survival compared to negative (assay media) and positive (Triton X-100; Sigma-Aldrich) control.

pKa predictions: The 2D structures of compounds monoamine **1e**, diamine **2e**, triamine **3e**, and diguanidine **4e** (in ChemDraw.cdx format) were imported into the Schrödinger software suite (2018–4 release) via the Maestro interface, and then prepared for further calculations using the LigPrep module [46]. The resulting 3D structures (neutral form) were then subjected to pKa prediction at pH 7.4 (solvent = H_2O) using the «sequential mode» of the Epik program [33,47]. In contrast to a standard pKa prediction, where the pKa of the individual functional groups are calculated, the sequential method removes/adds protons from/to the pH adjusted structure, and recalculates the pKa values after each step, which means that the effect of sequential ionization is taken into consideration in the pKa predictions.

4.4. Phase I metabolism

The murine liver microsomes (M9066, male rat, Sprague-Dawley) where purchased from Sigma-Aldrich. The derivatives investigated were all >95% pure as determined by reversed-phase (RP) high performance liquid chromatography (HPLC) with ultraviolet (UV) detection at 214 and 254 nm. Lidocaine was chosen as the positive control since its functional groups resembles the structure of the derivatives investigated. Lidocaine was synthesized in house. Acetonitrile and methanol were purchased from Sigma-Aldrich. Water was obtained from a Milli-Q rinsing system from Millipore.

Microsome incubations: The procedure for monitoring metabolic stability by murine liver microsomes was performed according to

Ackley et al. and Hansen et al. [30,48]. In brief, 90 μl of potassium phosphate buffer (100 mM, pH 7.4), 6 μL of freshly made NADPH regenerating system (consisting of 1.3 mM NADP, 3.3 mM glucose-6-phosphate, 0.4 U/mL glucose-6-phosphate dehydrogenase, 3.3 mM magnesium chloride in 100 mM phosphate buffer (pH 7.4)), and 1 μL of a newly thawed aqueous stock solution of substrate (100 μM) were added to 1.5 mL Eppendorf tubes. The tubes were centrifuged at low speed (2 s) and vortexed (5 s, medium strength) and placed in crushed ice while the liver microsomes solution (pooled from male Sprague–Dawley rats, 20 mg/mL) was thawed in a 37 °C water bath. Immediately after thawing and vortexing, 2.5 μL of microsomes was added each sample following centrifuging (2 s) and vortexing (5 s) and transferred to a 37 °C water bath (total sample volume 99.5 μL). The incubation tubes were quenched at given time points with 50 μL ice-cold methanol containing an internal standard (0.3 μg/mL propranolol hydrochloride), capped, vortexed, and put on ice for 1 h. The time points for **2e**, **2g**, and **2i** were 0, 5, 10, 15, 25, 45, 60 and 180 min, and for lidocaine 0, 5, 10, 25 and 40 min. The tubes were centrifuged at 13 000 rpm for 3 min at 4 °C. An aliquot of each sample (100 μL) were analysed by RP-HPLC and high-resolution mass spectrometry (HRMS). The control samples containing the derivative in question and the derivative plus the regenerating system were quenched at 180 min. The experiments were run in triplicates, and the quantification was run in duplicates. The samples were analysed within 24 h after preparation.

Calibration curves and recovery: Calibration curves were obtained for all derivatives from standard solutions in the concentration range 0.25–12.5 μM. The standard solutions were prepared using Milli-Q water as diluent. The calibration curves were prepared and run subsequently after the samples.

RP-HPLC analysis: The RP-HPLC analysis was performed using a Thermo Fischer Accela autosampler and a SunFire (Waters) TM 2.1 × 50 mm, 2.5 μm d_p, C_{18} column coupled to an Accela pump. The column heater was set to 40 °C and the autosampler at 4 °C. The mobile phase consisted of A (0.1% formic acid in Milli-Q water) and B (0.1% formic acid in acetonitrile). The following composition was used: 2% B for 2 min; a linear gradient of 2–50% B over 3 min; then 90% B for 1 min) The injection volume was 5 μL and the flow rate 400 μL min^{-1}. Flow was directed to waste at 0–1.5 min.

Mass spectrometry analysis of metabolites: A Thermo LTQ Orbitrap XL mass spectrometer was coupled to the RP-HPLC through an electrospray ionization (ESI) interphase and operated in the positive ion mode for quantitative analysis. The instrument was operated in full scan mode for quantitative determination of the substrates **2e**, **2g**, **2i** and lidocaine and semi-quantitative determination of their corresponding metabolites. For detection of the metabolites in the incubated samples the instrument was operated in full scan mode with mass range of 125 or 130 to 700 (m/z) (resolution 30 000). The detected metabolites were further analysed by targeted MS2 scan with higher-energy collisional dissociation (HCD) fragmentation at 35 eV (resolution 7500). The following settings were used for the analyses: Sheath gas flow rate 70, auxiliary gas flow rate 10, sweep gas flow rate 10, spray voltage 4.5 kV, capillary temperature 330 °C, capillary voltage 37 V, and tube lens 80 V.

Statistical treatment of the data: Percentage of remaining derivatives were calculated based on the area under the curve (single ion chromatogram, protonated molecular ion) for the derivatives compared to the internal standard. Average and standard deviations were calculated based on the concentrations. Response factor of the metabolites were assumed to be equal to the unmetabolised derivatives, hence enabling a semi-quantitation of the metabolites.

Acknowledgments

The study was funded by the Research Council of Norway (grant no. 214493) and UiT – The Arctic University of Norway (project no. A23260). We also thank the MABIT programme (grant no. BS0068) for funding screening against clinical isolates. The authors thank senior engineer Jostein Johansen (UiT) for help with MS analysis, professor Ørjan Samuelsen (K-Res/UNN) for giving us access to the multi-drug resistant clinical isolates, and engineers Alena Didriksen (UNN) and Hege Devold (UiT), and PhD student Eric Juskewitz (UiT) for their technical assistance with MIC screening. We also thank senior engineers Marte Albrigtsen and Kirsti Helland at Marbio (UiT) for their assistance with toxicity screening against HepG2 and MRC-5 cells, and associate professor Jon Våbenø (UiT) for valuable discussions.

Appendix A. Supplementary data

Supplementary data to this article can be found online at https://doi.org/10.1016/j.ejmech.2019.111671.

References

[1] O. Cars, A. Hedin, A. Heddini, The global need for effective antibiotics - moving towards concerted action, Drug Resist. Updates 14 (2) (2011) 68–69, https://doi.org/10.1016/j.drup.2011.02.006.
[2] L. Freire-Moran, B. Aronsson, C. Manz, I.C. Gyssens, A.D. So, D.L. Monnet, O. Cars, E.-E.W. Group, Critical shortage of new antibiotics in development against multidrug-resistant bacteria-Time to react is now, Drug Resist. Updates 14 (2) (2011) 118–124, https://doi.org/10.1016/j.drup.2011.02.003.
[3] A. Cassini, L.D. Högberg, D. Plachouras, A. Quattrocchi, A. Hoxha, G.S. Simonsen, M. Colomb-Cotinat, M.E. Kretzschmar, B. Devleesschauwer, M. Cecchini, D.A. Ouakrim, T.C. Oliveira, M.J. Struelens, C. Suetens, D.L. Monnet, B.o.A.C. Group, Attributable deaths and disability-adjusted life-years caused by infections with antibiotic-resistant bacteria in the EU and the European Economic Area in 2015: a population-level modelling analysis, Lancet Infect. Dis. 19 (1) (2019) 56–66, https://doi.org/10.1016/s1473-3099(18)30605-4.
[4] T. Kostyanev, M.J.M. Bonten, S. O'Brien, H. Steel, S. Ross, B. Francois, E. Tacconelli, M. Winterhalter, R.A. Stavenger, A. Karlén, S. Harbarth, J. Hackett, H.S. Jafri, C. Vuong, A. MacGowan, A. Witschi, G. Angyalosi, J.S. Elborn, R. deWinter, H. Goossens, The Innovative Medicines Initiative's New Drugs for Bad Bugs programme: European public-private partnerships for the development of new strategies to tackle antibiotic resistance, J. Antimicrob. Chemother. 71 (2) (2016) 290–295, https://doi.org/10.1093/jac/dkv339.
[5] V.L. Simpkin, M.J. Renwick, R. Kelly, E. Mossialos, Incentivising innovation in antibiotic drug discovery and development: progress, challenges and next steps, J. Antibiot. (Tokyo) 70 (12) (2017) 1087–1096, https://doi.org/10.1038/ja.2017.124.
[6] T. Hansen, D. Ausbacher, G.E. Flaten, M. Havelkova, M.B. Strøm, Synthesis of cationic antimicrobial $\beta^{2,2}$-amino acid derivatives with potential for oral administration, J. Med. Chem. 54 (3) (2011) 858–868, https://doi.org/10.1021/jm101327d.
[7] D. Ausbacher, A. Fallarero, J. Kujala, A. Määttänen, J. Peltonen, M.B. Strøm, P.M. Vuorela, *Staphylococcus aureus* biofilm susceptibility to small and potent $\beta^{2,2}$-amino acid derivatives, Biofouling 30 (1) (2014) 81–93, https://doi.org/10.1080/08927014.2013.847924.
[8] T. Hansen, T. Alst, M. Havelkova, M.B. Strøm, Antimicrobial activity of small β-peptidomimetics based on the pharmacophore model of short cationic antimicrobial peptides, J. Med. Chem. 53 (2) (2010) 595–606, https://doi.org/10.1021/jm901052r.
[9] L. Hanski, D. Ausbacher, T.M. Tiirola, M.B. Strøm, P.M. Vuorela, Amphipathic $\beta^{2,2}$-amino acid derivatives suppress infectivity and disrupt the intracellular replication cycle of *Chlamydia pneumoniae*, PLoS One 11 (6) (2016), e0157306, https://doi.org/10.1371/journal.pone.0157306.
[10] T. Hansen, D. Ausbacher, Z.G. Zachariassen, T. Anderssen, M. Havelkova, M.B. Strøm, Anticancer activity of small amphipathic $\beta^{2,2}$-amino acid derivatives, Eur. J. Med. Chem. 58 (2012) 22–29. https://doi.org/10.1016/j.ejmech.2012.09.048.
[11] D. Ausbacher, G. Svineng, T. Hansen, M.B. Strøm, Anticancer mechanisms of action of two small amphipathic $\beta^{2,2}$-amino acid derivatives derived from antimicrobial peptides, Biochim. Biophys. Acta 1818 (11) (2012) 2917–2925, https://doi.org/10.1016/j.bbamem.2012.07.005.
[12] M. Zasloff, Antimicrobial peptides of multicellular organisms, Nature 415 (6870) (2002) 389–395, https://doi.org/10.1038/415389a.
[13] A.A. Bahar, D. Ren, Antimicrobial peptides, Pharmaceuticals 6 (12) (2013) 1543–1575, https://doi.org/10.3390/ph6121543.
[14] R.M. Epand, R.F. Epand, Domains in bacterial membranes and the action of antimicrobial agents, Mol. Biosyst. 5 (6) (2009) 580–587, https://doi.org/

10.1039/b900278m.
[15] K.A. Brogden, Antimicrobial peptides: pore formers or metabolic inhibitors in bacteria? Nat. Rev. Microbiol. 3 (3) (2005) 238–250, https://doi.org/10.1038/nrmicro1098.
[16] M.B. Strøm, B.E. Haug, M.L. Skar, W. Stensen, T. Stiberg, J.S. Svendsen, The pharmacophore of short cationic antibacterial peptides, J. Med. Chem. 46 (9) (2003) 1567–1570, https://doi.org/10.1021/jm0340039.
[17] P. Teng, D. Huo, A. Nimmagadda, J. Wu, F. She, M. Su, X. Lin, J. Yan, A. Cao, C. Xi, Y. Hu, J. Cai, Small antimicrobial agents based on acylated reduced amide scaffold, J. Med. Chem. 59 (17) (2016) 7877–7887, https://doi.org/10.1021/acs.jmedchem.6b00640.
[18] C. Ghosh, G.B. Manjunath, P. Akkapeddi, V. Yarlagadda, J. Hoque, D.S.S.M. Uppu, M.M. Konai, J. Haldar, Small molecular antibacterial peptoid mimics: the simpler the better!, J. Med. Chem. 57 (4) (2014) 1428–1436, https://doi.org/10.1021/jm401680a.
[19] R.P. Dewangan, S. Joshi, S. Kumari, H. Gautam, M.S. Yar, S. Pasha, N-terminally modified linear and branched spermine backbone dipeptidomimetics against planktonic and sessile methicillin-resistant *Staphylococcus aureus*, Antimicrob. Agents Chemother. 58 (9) (2014) 5435–5447, https://doi.org/10.1128/AAC.03391-14.
[20] R.N. Murugan, B. Jacob, E.H. Kim, M. Ahn, H. Sohn, J.H. Seo, C. Cheong, J.K. Hyun, K.S. Lee, S.Y. Shin, J.K. Bang, Non hemolytic short peptidomimetics as a new class of potent and broad-spectrum antimicrobial agents, Bioorg. Med. Chem. Lett 23 (16) (2013) 4633–4636, https://doi.org/10.1016/j.bmcl.2013.06.016.
[21] B.E. Haug, W. Stensen, M. Kalaaji, Ø. Rekdal, J.S. Svendsen, Synthetic antimicrobial peptidomimetics with therapeutic potential, J. Med. Chem. **51** (14) (2008) 4306–4314, https://doi.org/10.1021/jm701600a.
[22] J. Isaksson, B.O. Brandsdal, M. Engqvist, G.E. Flaten, J.S.M. Svendsen, W. Stensen, A synthetic antimicrobial peptidomimetic (LTX 109): stereochemical impact on membrane disruption, J. Med. Chem. 54 (16) (2011) 5786–5795, https://doi.org/10.1021/jm200450h.
[23] P. Gunasekaran, G. Rajasekaran, E.H. Han, Y.H. Chung, Y.J. Choi, Y.J. Yang, J.E. Lee, H.N. Kim, K. Lee, J.S. Kim, H.J. Lee, E.J. Choi, E.K. Kim, S.Y. Shin, J.K. Bang, Cationic amphipathic triazines with potent anti-bacterial, anti-inflammatory and anti-atopic dermatitis properties, Sci. Rep. 9 (1) (2019) 1292, https://doi.org/10.1038/s41598-018-37785-z.
[24] F. Sgolastra, B.M. deRonde, J.M. Sarapas, A. Som, G.N. Tew, Designing mimics of membrane active proteins, Acc. Chem. Res. 46 (12) (2013) 2977–2987, https://doi.org/10.1021/ar400066v.
[25] H.D. Thaker, A. Som, F. Ayaz, D. Lui, W. Pan, R.W. Scott, J. Anguita, G.N. Tew, Synthetic mimics of antimicrobial peptides with immunomodulatory responses, J. Am. Chem. Soc. 134 (27) (2012) 11088–11091, https://doi.org/10.1021/ja303304j.
[26] H.D. Thaker, A. Cankaya, R.W. Scott, G.N. Tew, Role of amphiphilicity in the design of synthetic mimics of antimicrobial peptides with gram-negative activity, ACS Med. Chem. Lett. 4 (5) (2013) 481–485, https://doi.org/10.1021/ml300307b.
[27] D. Liu, S. Choi, B. Chen, R.J. Doerksen, D.J. Clements, J.D. Winkler, M.L. Klein, W.F. DeGrado, Nontoxic membrane-active antimicrobial arylamide oligomers, Angew. Chem., Int. Ed. Engl. 43 (9) (2004) 1158–1162, https://doi.org/10.1002/ange.200352791.
[28] G.N. Tew, D. Liu, B. Chen, R.J. Doerksen, J. Kaplan, P.J. Carroll, M.L. Klein, W.F. DeGrado, De novo design of biomimetic antimicrobial polymers, Proc. Natl. Acad. Sci. U. S. A. 99 (8) (2002) 5110–5114, https://doi.org/10.1073/pnas.082046199.
[29] A. Koivuniemi, A. Fallarero, A. Bunker, Insight into the antimicrobial mechanism of action of $\beta^{2,2}$-amino acid derivatives from molecular dynamics simulation: dancing the can-can at the membrane surface, Biochim. Biophys. Acta Biomembr. 1861 (11) (2019), 183028, https://doi.org/10.1016/j.bbamem.2019.07.016.
[30] T. Hansen, M.K. Moe, T. Anderssen, M.B. Strøm, Metabolism of small antimicrobial $\beta^{2,2}$-amino acid derivatives by murine liver microsomes, Eur. J. Drug Metab. Pharmacokinet. 37 (3) (2012) 191–201, https://doi.org/10.1007/s13318-012-0086-9.
[31] L.B. Rice, Federal funding for the study of antimicrobial resistance in nosocomial pathogens: no ESKAPE, J. Infect. Dis. 197 (8) (2008) 1079–1081, https://doi.org/10.1086/533452.
[32] M.H. Paulsen, M. Engqvist, D. Ausbacher, M.B. Strøm, A. Bayer, Efficient and scalable synthesis of α,α-disubstituted β-amino amides, Org. Biomol. Chem. 14 (31) (2016) 7570–7578, https://doi.org/10.1039/c6ob01219a.
[33] J.C. Shelley, A. Cholleti, L.L. Frye, J.R. Greenwood, M.R. Timlin, M. Uchimaya, Epik: a software program for pKa prediction and protonation state generation for drug-like molecules, J. Comput. Aided. Mol. 21 (12) (2007) 681–691, https://doi.org/10.1007/s10822-007-9133-z.
[34] T. Ito, Y. Katayama, K. Hiramatsu, Cloning and nucleotide sequence determination of the entire mec DNA of pre-methicillin-resistant *Staphylococcus aureus* N315, Antimicrob. Agents Chemother. 43 (6) (1999) 1449–1458, https://doi.org/10.1128/aac.43.6.1449.
[35] T. Ito, Y. Katayama, K. Asada, N. Mori, K. Tsutsumimoto, C. Tiensasitorn, K. Hiramatsu, Structural comparison of three types of staphylococcal cassette chromosome mec integrated in the chromosome in methicillin-resistant *Staphylococcus aureus*, Antimicrob. Agents Chemother. 45 (5) (2001) 1323–1336, https://doi.org/10.1128/AAC.45.5.1323-1336.2001.
[36] T. Ito, X.X. Ma, F. Takeuchi, K. Okuma, H. Yuzawa, K. Hiramatsu, Novel type V staphylococcal cassette chromosome mec driven by a novel cassette chromosome recombinase, ccrC. *Antimicrob. Agents Chemother.* 48 (7) (2004) 2637–2651, https://doi.org/10.1128/AAC.48.7.2637-2651.2004.
[37] The Norwegian National Advisory Unit on Detection of Antimicrobial Resistance (K-res), University Hospital of North Norway – UNN.
[38] Ø. Samuelsen, M.A. Toleman, A. Sundsfjord, J. Rydberg, T.M. Leegaard, M. Walder, A. Lia, T.E. Ranheim, Y. Rajendra, N.O. Hermansen, T.R. Walsh, C.G. Giske, Molecular epidemiology of metallo-β-lactamase-producing *Pseudomonas aeruginosa* isolates from Norway and Sweden shows import of international clones and local clonal expansion, Antimicrob. Agents Chemother. 54 (1) (2010) 346–352, https://doi.org/10.1128/AAC.00824-09.
[39] N. Karah, B. Haldorsen, N.O. Hermansen, Y. Tveten, E. Ragnhildstveit, D.H. Skutlaberg, S. Tofteland, A. Sundsfjord, Ø. Samuelsen, Emergence of OXA-carbapenemase- and 16S rRNA methylase-producing international clones of *Acinetobacter baumannii* in Norway, J. Med. Microbiol. 60 (4) (2011) 515–521, https://doi.org/10.1099/jmm.0.028340-0.
[40] Ø. Samuelsen, S. Overballe-Petersen, J.V. Bjørnholt, S. Brisse, M. Doumith, N. Woodford, K.L. Hopkins, B. Aasnæs, B. Haldorsen, A. Sundsfjord, C.P.E. Norwegian Study Group on, Molecular and epidemiological characterization of carbapenemase-producing Enterobacteriaceae in Norway, 2007 to 2014, PLoS One 12 (11) (2017), e0187832, https://doi.org/10.1371/journal.pone.0187832.
[41] H.J. Böhm, D. Banner, S. Bendels, M. Kansy, B. Kuhn, K. Müller, U. Obst-Sander, M. Stahl, Fluorine in medicinal Chemistry, Chembiochem 5 (5) (2004) 637–643, https://doi.org/10.1002/cbic.200301023.
[42] E.A. Dixon, A. Fischer, F.P. Robinson, Preparation of a series of substituted fluoromethylnaphthalenes, Can. J. Chem. 59 (1981) 2629–2641, https://doi.org/10.1139/v81-379, 17.
[43] C.a.L.S. Institute, CLSI Document M07-A9, in: Methods for Dilution Antimicrobial Susceptibility Tests for Bacteria that Grow Aerobically. Approved Standard, 9 ed. vol. 32, CLSI, Wayne, PA, 2012. *No. 2. Wayne, PA, USA, 2012*.
[44] E.M. Igumnova, E. Mishchenko, T. Haug, H.M. Blencke, J.U.E. Sollid, E.G.A. Fredheim, S. Lauksund, K. Stensvåg, M.B. Strøm, Synthesis and antimicrobial activity of small cationic amphipathic aminobenzamide marine natural product mimics and evaluation of relevance against clinical isolates including ESBL-CARBA producing multi-resistant bacteria, Bioorg. Med. Chem. 24 (22) (2016) 5884–5894, https://doi.org/10.1016/j.bmc.2016.09.046.
[45] V. Tørfoss, D. Ausbacher, C.d.A. Cavalcanti-Jacobsen, T. Hansen, B.O. Brandsdal, M. Havelkova, M.B. Strøm, Synthesis of anticancer heptapeptides containing a unique lipophilic $\beta^{2,2}$-amino acid building block, J. Pept. Sci. 18 (3) (2012) 170–176, https://doi.org/10.1002/psc.1434.
[46] Schrödinger Release 2019-3, *LigPrep, Schrödinger*, LLC, 2019. New York, NY.
[47] Schrödinger Release 2018-4, Epik, Schrödinger, *LLC*, 2018. New York, NY.
[48] D.C. Ackley, K.T. Rockich, T.R. Baker, Metabolic stability assessed by liver microsomes and hepatocytes, in: Z. Yan, G.W. Caldwell (Eds.), Methods in Pharmacology and Toxicology - Optimization in Drug Discovery: in Vitro Methods, Humana Press, Totowa, NJ, 2004, pp. 151–162, https://doi.org/10.1385/1-59259-800-5:151.